

# Proton Exchange Membrane Fuel Cell Combined with Battery and Flywheel Energy Storage for Sustainable Power and Clean Electric Trike Vehicle

Ganesha Tri Chandrasa<sup>1</sup>, Heri Suryoatmojo<sup>2\*</sup>, Barman Tambunan<sup>3</sup>, Tata Sutardi<sup>4</sup>, Taurista Perdana Syawitri<sup>5</sup>

<sup>1,2</sup>Dept. of Electrical Engineering, Institut Teknologi Sepuluh Nopember, Surabaya, East Java, 60111, Indonesia

<sup>1,3,4,5</sup>Research Center for Energy Conversion and Conservation, National Research and Innovation Agency, B. J. Habibie Science and Technology Park, South Tangerang, Banten, 15314, Indonesia

Email: <sup>1</sup>gane001@brin.go.id, <sup>2</sup>suryomgt@ee.its.ac.id, <sup>3</sup>barm001@brin.go.id, <sup>4</sup>tata012@brin.go.id, <sup>5</sup>taur003@brin.go.id

\*Corresponding Author

**Abstract**—An electric personal three-wheeler, referred to as the Reverse Trike Electric Vehicle (RTEV), has been developed as a forward-looking solution for clean transportation within communities. This innovative vehicle integrates multiple energy storage systems, including the mechanical energy of a flywheel, the chemical energy of a hydrogen (H<sub>2</sub>) fuel cell system, and the chemical energy stored in a lithium-ion battery. The vehicle is powered by a 500-watt, 48-volt platform that incorporates a DC brushless electric motor, a battery, and a fuel-cell. Hydrogen is stored in two steel tube containers filled with ultra-high purity (UHP) hydrogen, with output pressure ranging from 10 to 35 psi. The lithium battery pack features a configuration of 13 series and 3 parallel (13S3P) cells, assembled using 18650-sized lithium-ion cells. Additionally, two flywheels of varying mass were utilized in the design. The prototype underwent testing both indoors on a dynamometer test bed and outdoors on community roads for analysis. The results from these tests clearly demonstrate the contributions of each energy storage system to the vehicle's power traction and distance performance, showcasing the effectiveness of this multi-faceted approach to clean transportation.

**Keywords**—Electric Vehicle; Hybrids Energy Storage; Fuel Cell; PEMFC; Lithium Battery; Flywheel Storage.

## I. INTRODUCTION

The transportation sector contributes significantly to global greenhouse gas emissions, prompting a worldwide transition towards renewable energy options, particularly in urban transportation [1]. Electric vehicles (EVs) have emerged as a promising solution for reducing dependency on fossil fuels and mitigating environmental impact. Electric trikes—compact, three-wheeled vehicles—are becoming increasingly popular for short-distance urban transportation due to their energy efficiency, maneuverability, and low operating costs [2]. Despite their benefits, electric trikes have a number of challenges including a limited driving range, delayed recharging periods, and inefficient energy management [2]-[5].

While electric trikes offer a promising solution for urban transportation, current designs face significant challenges, particularly related to limited driving range, inefficient energy management, and delayed recharging times. The lack of an optimized hybrid energy system that can address both dynamic power demands and long-term efficiency remains a critical gap in existing research and development efforts.

These constraints are mostly due to the reliance on traditional battery systems, which deteriorate over time and have trouble controlling dynamic power demands [2]-[5]. In addition, Proton Exchange Membrane Fuel Cells (PEMFCs) combined with sophisticated energy storage devices like flywheels and batteries represent a potentially viable alternative. This hybrid technique has the potential to improve the energy density and overall efficiency of electric tricycle vehicles, paving the way for more sustainable urban mobility.

Through an electrochemical reaction, PEMFCs transform hydrogen's chemical energy into electrical energy, using water as a byproduct [6]-[7]. They are a desirable option for clean transportation due to their great efficiency and low emission levels [6][8]. The practicality of PEMFCs for commercial applications has been greatly increased by recent developments in the technology, such as advances in catalyst materials and membrane durability [9].

However, one of the most significant issues associated with PEMFCs is their susceptibility to energy changes during operation [6]. These oscillations are often caused by the dynamic nature of power demand in many applications, particularly in cars, where energy consumption can fluctuate dramatically depending on speed, load, and environmental conditions [10]. While PEMFCs are effective at turning hydrogen into energy, they do not respond quickly to abrupt changes in power requirements [10]. This causes performance difficulties including voltage drops or spikes, which can have a severe influence on both fuel cell efficiency and overall system stability [6][11]. Furthermore, these variations can induce wear and degradation in fuel cell components over time, limiting their lifespan and dependability [6][11]. To overcome these issues, energy storage devices such as batteries, superconductors, or flywheel energy storage systems (FESS) [12] are frequently used with PEMFCs to buffer energy output, assuring a consistent and dependable power supply while operating.

The combination of PEMFCs and a lithium-ion battery creates a hybrid system in which the battery provides short bursts of power at peak loads while the fuel cell offers long-term energy [13]. This PEMFC-battery system optimizes the performance of the PEMFC by enabling it to run at its most



economical operating point, which is often a lower power output, while the battery handles changes in load demand [13]. Lithium-ion batteries are extensively employed in EVs due to their high energy density and ability to store significant quantities of energy relative to their weight, although they degrade after repeated charge and discharge cycles [14][15]. Urooj and Nasir have examined a number of hybrids PEMFC-battery systems and discovered that they increase the system's power density in addition to improving energy efficiency [16], which makes them appropriate for a variety of applications ranging from bigger commercial vehicles to light-duty vehicles like electric trikes. Their study showed that because the battery can manage peak loads, hybrid systems require smaller fuel cells, which decreases the system's overall cost [16]. Additionally, hybrid systems offer superior energy recovery during regenerative braking [17], which is especially advantageous for city cars with frequent stops and starts, such as electric trikes. The vehicle's energy efficiency is further increased by the lithium-ion battery's ability to swiftly store the recovered energy and release it when needed [17]. Despite the potential of PEMFC-lithium ion battery hybrid systems, significant challenges remain. One of the most significant issues is the complexity of the energy management system (EMS) necessary to optimize power flow between the fuel cell and the battery. To guarantee that the hybrid system functions effectively in a variety of driving scenarios, effective EMS algorithms are required. Research has demonstrated that by dynamically modifying the power output of every component in real-time, sophisticated control techniques like model predictive control (MPC) can enhance the performance of hybrid systems [18].

The performance of EVs is further improved by integrating PEMFC-battery technologies with FESS, which improves energy recovery during regenerative braking and offers high-power bursts [19-23]. In this hybrid configuration, the PEMFC serves as the primary energy source, providing constant power for long distance travel. The lithium-ion Battery supports the PEMFC by storing excess energy for later use and delivering rapid bursts of power during acceleration or high-demand scenarios. Meanwhile, the flywheel enhances the system by enabling quick absorption and release of energy, especially during regenerative braking or other transient conditions. [24]. Previous study has shown that hybrid PEMFC-battery-flywheel systems greatly enhance energy efficiency and overall hybrid small car performance, especially in urban driving settings where frequent stops and starts put a strain on energy storage systems [25]. For extended periods of high demand, the battery supplies the energy storage required, while the flywheel efficiently handles the brief, high-power needs connected to quick acceleration and deceleration [25]. This hybrid system is particularly well-suited for urban environments, where frequent stops and starts place a significant strain on traditional energy storage systems. By leveraging the strengths of the PEMFC, lithium-ion battery, and flywheel, the electric trike can offer enhanced efficiency and performance in the demanding conditions of city traffic.

This study focused on the development and implementation of a hybrid energy system for electric trike

applications, integrating flywheel energy storage, lithium-ion batteries, and PEMFCs. Building on a previous study by the first author [26], this work introduces significant modifications to the prototype by increasing the flywheel mass and redesigning the electric trike platform, leading to improved energy efficiency, range, and overall performance. Both indoor dynamometer tests and outdoor testing were conducted to assess the prototype vehicle performances.

This work presents the development of a Reverse Trike Electric Vehicle (RTEV), a novel solution aimed at advancing clean transportation for urban environments. The RTEV integrates multiple energy storage systems to address the challenges of limited driving range and energy efficiency in traditional electric vehicles.

By advancing the development of more efficient and sustainable energy solutions for electric trikes, this study aims to contribute to the broader transition towards cleaner, more sustainable urban transportation options, aligning with global efforts to reduce greenhouse gas emissions and dependence on fossil fuels.

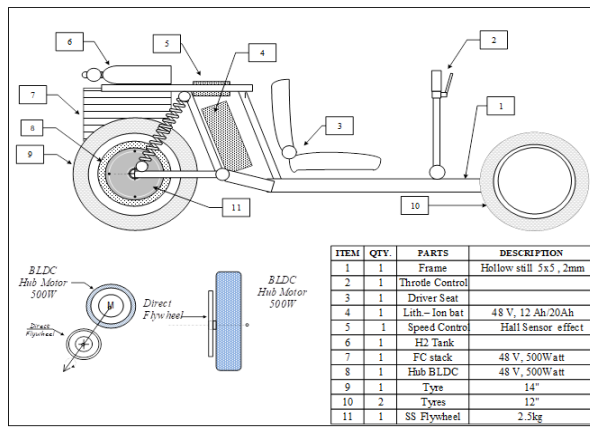
## II. EASE MATERIAL AND METHODS

This paper presents the results of extensive experiments conducted by the authors, building upon previous work of involving a flywheel with a mass of 2.5 kg used in 2022 [26] (see Fig. 1a). The RTEV is powered by a 500-watt, 48-volt platform that combines a DC brushless electric motor with three energy sources: a lithium-ion battery, a hydrogen fuel cell system, and a flywheel energy storage system.

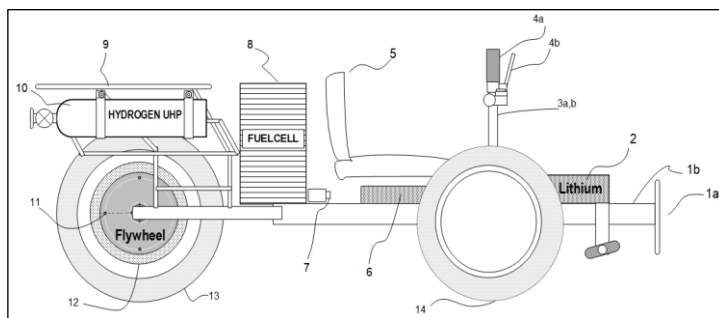
For this study, a heavier flywheel with a mass of 3.2 kg has been utilized, as detailed in this study. Moreover, a new platform has been designed and constructed to enhance stability, featuring a repositioning of critical components, including two hydrogen tanks and a fuel cell system, to create a more stable and secure setup during maneuvers (see Fig. 1b). Experiments were conducted on a dynamometer test bed, with all data recorded using a PC logger, power meter, and dynamometer.

### A. Battery Energy Storage

For research purposes, a customized battery pack has been made according to schematic diagram of the proposed design as shown in Fig. 2. The battery pack was assembled from 39 Samsung tubular cells of the INR18650-35E type. Energy capacity per cell is 3.5 Ah, with nominal voltage about 3.6V/cell to 4.2 Volt maximum Voltage and has 8000 mA discharge current capability. Hence, cells were configured in 13 series, and 3 parallel, resulted in total maximum 54.6 Volt and 10.5 Ah or 573.3 Watthour energy stored in the battery pack. For safety reasons battery pack is assembled with a standard battery management system ("Daly" BMS) that available in the market, its can control each battery cell to ensure safety, by protecting cells from overcurrent, over-charge, over-discharge, short circuit, thermal management and balance of cells, [27]. The BMS can handle maximum 50 Ampere of discharge current and 25 Ampere charge current.



(a)



(b)

Fig. 1. (a) The first prototype electric trike vehicle platform design, with 2.5 kg flywheel [26] and (b) Platform design of the new reverse electric trike vehicle with 3.2 kg flywheel mass

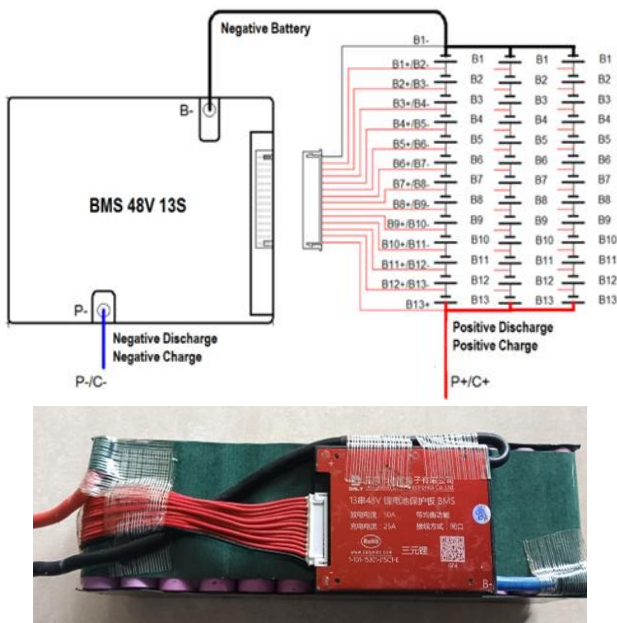


Fig. 2. Design schematic diagram and assembled of the battery pack

**B. Hydrogen Fuel Cells**

To convert hydrogen into electrical energy suitable for powering transportation modes such as electric vehicles, a fuel cell system is necessary. In addition to hydrogen, oxygen from the air must also be supplied to the system stacks. The reaction between hydrogen and oxygen facilitates the movement of electrons from the anode to the cathode,

generating electric current that can directly operate electrical loads, such as an electric motor [28]. Any excess power generated can be stored in batteries or supercapacitors in the electric vehicle.

The fuel cell system must effectively manage hydrogen inlet pressure and temperature, as higher power output requires higher pressure, which in turn generates increased temperatures. However, excessive heat can damage the cell materials. One inherent characteristic of fuel cells is polarization loss, which limits their ability to provide power during sudden acceleration or deceleration [29][30]. To address this limitation, this research implements a combination of energy sources, integrating a hydrogen fuel cell with lithium batteries for chemical energy storage and incorporating a flywheel for mechanical energy storage.

Fig. 3(a) illustrates the reactions occurring within the fuel cell stack, producing environmentally friendly byproducts, including heat, air, and water. The electrical circuit equivalent of the fuel cell stack is depicted in Fig. 3(b), while Fig. 3(c) shows the energy flow from the fuel cell to the load and battery. Additionally, Fig. 4(a) outlines the fuel cell's characteristics, including various losses [30]-[32]. In this study, the fuel cell system used for the experiment was a 500 W PEMFC (PS500), which is a discontinued product from the former "H Power Corp". Fig. 4(b) presents the fuel cell system utilized in the experiment, comprising the fuel cell stack, cooling fans, air compressor, and controller, all housed within a compact enclosure.

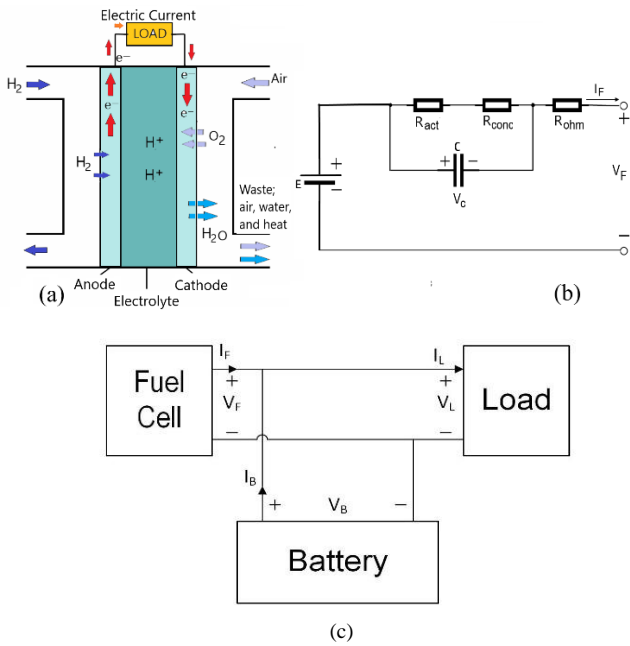


Fig. 3. (a) Reaction inside fuel cell stack, (b) Electric circuit equivalent of fuel cell [29]-[30], and (c) fuel cell and battery

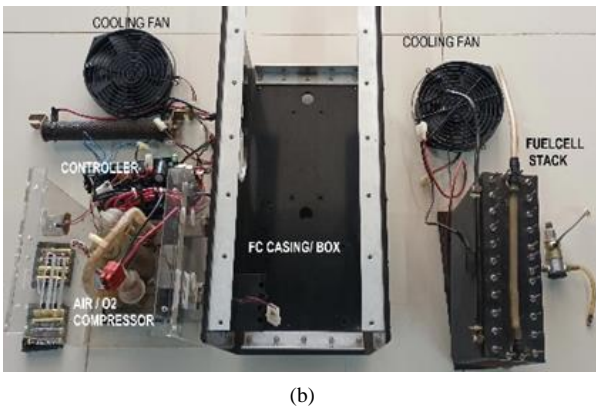
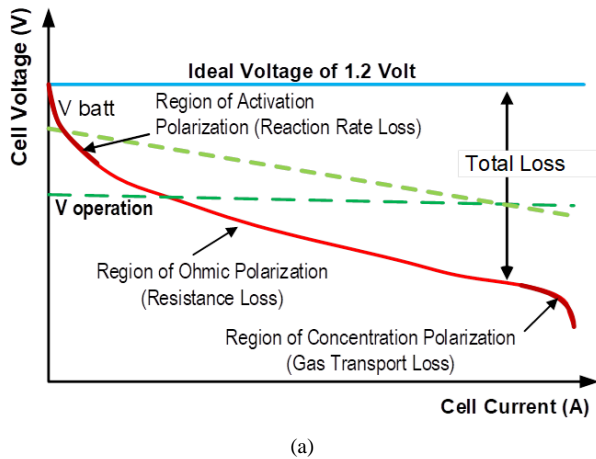


Fig. 4. (a) Fuel cell characteristic due to some losses [30], [31], [32] and (b) Fuel cell system parts

C. Flywheel Energy Storage Technology & Material

Flywheel technology has been utilized for many years in applications such as old locomotives, ships, and power plants, primarily for storing kinetic energy for later use. Numerous studies have highlighted the benefits of adopting high-speed Flywheel Energy Storage (FES) systems, with

efficiency levels reported to range from 50% to 89% in vacuum conditions [22][33]. Flywheels are often considered cleaner and more durable than electrochemical batteries. In this research, efforts were focused on developing a FES system for a 500Watt BLDC motor, which has a limited rotational speed of less than 1000 rpm. The FES used in this study falls under the category of low-speed flywheel systems. Fig. 5 illustrates a flywheel with mass (*m*) and radius (*r*) rotating at a speed ( $\omega$ ) around its axis.

The following (1) was used to calculate the kinetic energy of a flywheel.

$$E_k = \frac{1}{2} I \omega^2 \tag{1}$$

where *I* is the moment of inertia around the axis of rotation. A higher moment of inertia results in lower acceleration when torque is applied, meaning a greater energy moment leads to slower acceleration.

For a solid cylinder flywheel, the moment of inertia was calculated using (2).

$$I = \frac{1}{2} m r^2 \tag{2}$$

For a thin cylinder, the moment of inertia was calculated using (3).

$$I = m r^2 \tag{3}$$

For a hollow cylinder, the moment of inertia was calculated using (4).

$$I = \frac{1}{2} m (r_{outer}^2 + r_{inner}^2) \tag{4}$$

During the rotation of a flywheel, a force called centrifugal force (*F*) is generated, acting outward from the centre of the axis. The (5) was applied for calculating this force.

$$F = m \omega^2 r \tag{5}$$

Different materials can be used to fabricate flywheels, depending on the application. For instance, tin is often used for small or micro flywheels, such as those in toys or watches, while cast iron has been used in steam trains and power plants, aluminum and steel are commonly used in internal combustion engine vehicles. Additionally, high-strength steel or composite materials are often employed for energy storage systems in braking applications [33][34].

The efficiency of a flywheel is determined by the amount of energy stored per unit of mass, with stored energy increasing as rotational speed rises. However, as the speed increases, so does the stress level on the material. Each material has a tensile strength limit, beyond which it may fail. Stainless steel, with a density of 7.982 kg/m<sup>3</sup>, was selected for the prototype flywheel in this research due to the availability of raw material in the local market, affordable cost, and easy to lathe.

#### D. Power and Energy Demands

In designing an electric trike, several formulas were used to calculate the power and energy required to move the vehicle during a trip. Factors such as the trike's mass, speed, and road topology significantly influence these calculations. Fig. 6 illustrates the forces that act on the vehicle throughout its journey.

To calculate the power required for the vehicle to maintain a specific constant velocity ( $v$ ) in m/s, engine power ( $P$ ) in Watt, the formula (6) is used.

$$P = \frac{F_v v}{\eta} \quad (6)$$

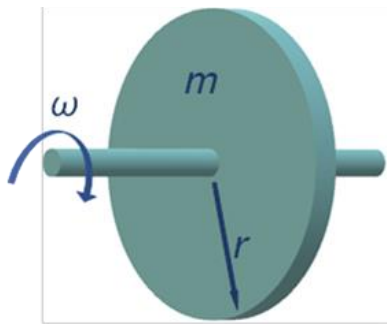


Fig. 5. Solid disc flywheel

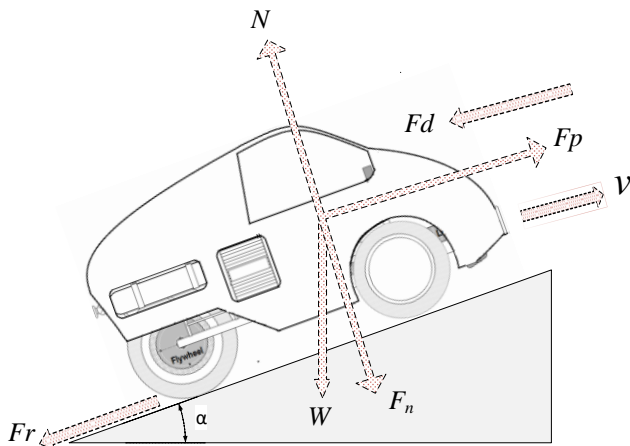


Fig. 6. Forces acting on a vehicle

where  $F_v$  is the total force acting on the vehicle (Newton) and represents the efficiency of the transmission (%). The total force acting on the vehicle consists of several contributing forces as described in (7).

$$F_r = F_r + F_p + F_d \quad (7)$$

For  $F_r$  is the rolling resistance force (N), which is the resistance encountered by the trike's tires as they roll on a surface. It was calculated using (8).

$$F_r = \mu_k N = \mu_k mg \quad (8)$$

where  $\mu_k$  is the rolling resistance coefficient,  $N$  is the normal force (in Newtons),  $m$  is the mass of the vehicle (kg), and  $g$  is the acceleration due to the gravity ( $m/s^2$ ).  $F_p$  is the gradient resistance force (N), representing the pulling force required to move the trike uphill. It is influenced by the elevation angle ( $\alpha$ ) and was calculated by using (9).

$$F_p = mgsin\alpha \quad (9)$$

$F_d$  is the aerodynamic drag resistance force (N), which is the force exerted by air resistance against the moving vehicle. It was calculated based on (10) below.

$$F_d = \frac{1}{2} \mu_d \rho A v^2 \quad (10)$$

where  $\mu_d$  is the drag coefficient,  $\rho$  is the air density ( $kg/m^3$ ), and ( $A$ ) is the frontal area of the vehicle ( $m^2$ ). The frontal area was calculated as the product of the vehicle's front width ( $w$ ), and front height ( $h$ ),

$$A = wh \quad (11)$$

To estimate the fuel-cell and battery capacity required for the trike, the total energy consumption  $E$ , (Wh), was calculated using (12) or (13).

$$E = Pt \quad (12)$$

$$E = \frac{Ps}{v} \quad (13)$$

Where  $t$  is the duration of use (hours). Alternatively, the energy consumption can also be determined based on the distance travelled ( $s$ ) and velocity as shown in (13). Table I presents a spreadsheet of the simulation design of the designed vehicle, incorporating specific parameters such as vehicle mass, speed, and road incline, to calculate the required output forces.

#### E. Experimental Method

This study evaluated the prototype of an electric trike vehicle under two distinct environmental conditions: outdoor and indoor testing (as shown in Fig. 7(a) and Fig. 7(b), respectively). The indoor testing was conducted on a dynamometer test bed to assess the effects of flywheel mass, PEMFC pressure, and battery performance on the vehicle's speed, torque, and power output. In addition, outdoor testing took place on community streets within the B. J. Habibie Science and Technology Park in South Tangerang, Indonesia. The outdoor testing aimed to evaluate the system's robustness in real-world conditions, focusing on optimal power delivery, energy recovery, and overall system durability. It also provided data on the vehicle's achievable speed and distance in practical scenario.

TABLE I. SIMULATION DESIGN OF EV PLATFORMS' POWER DEMAND

DESIGN CALCULATION							
<b>Assumption</b>							
	a. All unit are in metric						
	b. Vehicle runs in constant speed						
	c. Type of road is asphalt						
	d. Efficiency in the transmission is 100%						
<b>1</b>	<b>Vehicle Specification</b>						
	Mass of vehicle / gross vehicle weight	$m$	:	75	kg	75	kg
	Velocity	$v$	:	35	km/h	12	km/h
	Elevation angle	$\alpha$	:	0	degrees	10	degrees
	Front width of the vehicle	$w$	:	0.8	m	0.8	m
	Front height of the vehicle	$h$	:	0.8	m	0.8	m
	Range Distance	$s$	:	40	km	17	km
<b>2</b>	<b>Constant Value</b>						
	Efficiency in the transmission	$\eta$	:	98	%	98	%
	Rolling resistance coefficient	$\mu_k$	:	0.004	-	0	-
	Acceleration of gravity	$g$	:	9.81	m/s <sup>2</sup>	9.81	m/s <sup>2</sup>
	Drag coefficient	$\mu_d$	:	0.9	-	0.9	-
	Density of air	$\rho$	:	1.2	kg/m <sup>3</sup>	1.2	kg/m <sup>3</sup>
<b>3</b>	<b>Output</b>						
	Rolling Resistance Force	$F_r$	:	2.943	N	2.94	N
	Gradient Resistance Force	$F_p$	:	0	N	128	N
	Aerodynamic Drag Resistance Force	$F_d$	:	32.67	N	3.84	N
	Total force acting on the vehicle	$F$	:	35.61	N	135	N
	Engine power	$P$	:	353.27	W	458	W
	Energy consumption	$E$	:	403.74	Wh	648	Wh
	<b>Battery Type</b>	$LFP$	:	120	Wh/kg		
	<b>Mass of battery</b>		:	3.36	kg	5	kg



Fig. 7. (a) Outdoor and (b) Indoor test of the new platform trike

### III. RESULTS AND DISCUSSIONS

The findings of this study provide a thorough examination of the electric trike vehicle's performance under both controlled (indoor) and real-world (outdoor) situations. The data from these tests show how major variables like flywheel mass, PEMFC pressure, and battery integration affect the vehicle's speed, torque, and power output. This section presents and discusses the findings in terms of their implications for energy efficiency, power stability, and system durability. Indoor dynamometer findings are compared to outdoor performance data to assess the hybrid energy storage system's overall effectiveness in supplying sustained power, energy recovery, and vehicle range.

#### A. Power System Performance Benchmark

The simulation design, as shown in Table I, provides essential parameters for optimizing the power components of the vehicle to handle all acting forces. Based on the simulation results, with an assumed vehicle gross weight of 75 kg and a payload of 85 kg, an expected velocity of 35

km/h, and road inclinations ranging from 0 to 10 degrees, all forces can be managed by a 500 W BLDC motor. The required energy from the power sources is approximately 650 Wh.

To determine the optimal dimensions for the flywheels, the simulations were conducted as shown in Tables II and III, yielding different outputs based on variations in mass, size, and rotational speed. According to Table II, the first flywheel prototype was designed with a diameter ( $d$ ) of 180 mm and a mass of 2500 grams (2.5 kg). Meanwhile, Table 3 describes the second test with a larger flywheel, featuring a diameter of 200 mm and a mass of 3200 grams (3.2 kg).

As shown in Table III, the larger flywheel demonstrated an output of 0.877 J of kinetic energy and 3.57 kg of centrifugal force at 100 rpm, higher than those results for the old flywheel with 2.5 kg of mass. This is understandable as a higher mass of the flywheel contributes to increase centrifugal force due to its direct relationship in the formula (see (5)), resulting in greater stability, energy storage, and

performance in rotational systems. It also can be seen that at 600 rpm, the new flywheel produced 31.59 J of kinetic energy and 128.56 kg of centrifugal force, indicating it could propel the vehicle with a gross weight of 75 kg plus a passenger with 50-55 kg of weight. Meanwhile, the old flywheel could only handle the weight of vehicle with 15 kg passenger at this 600 rpm.

TABLE II. INPUT AND OUTPUT OF TESTS WITH FLYWHEEL 2500 GRAMS MASS [26]

No	Input (Flywheel Disc)			Output			
	$m$ (gram)	$d$ (mm)	rpm	Inertia (kgm <sup>2</sup> )	Kinetic energy (J)	Centrifugal force	
				$I$ $= \frac{1}{2}mr^2$	$E_k$ $= \frac{1}{2}I\omega^2$	Newtons	kg
1	2500	180	100	0.01	0.555	24.68	2.52
2	2500	180	200	0.01	2.222	98.72	10.07
3	2500	180	300	0.01	4.99	222.12	22.65
4	2500	180	400	0.01	8.88	394.89	40.27
5	2500	180	500	0.01	13.88	617.01	62.91
6	2500	180	600	0.01	19.99	888.49	90.6
7	2500	180	700	0.01	27.21	1209.3	123.32
8	2500	180	800	0.01	35.540	1579.5	161.07
9	2500	180	900	0.01	44.980	1999.1	203.85
10	2500	180	1000	0.01	55.531	2468	251.67
11	2500	180	1100	0.01	67.192	2986.3	304.52
12	2500	180	1200	0.01	79.65	3554.0	362.4
13	2500	180	1300	0.01	93.847	4171.0	425.32
14	2500	180	1400	0.01	108.84	4837.4	493.27
15	2500	180	1500	0.01	129.94	5553.1	566.26

TABLE III. INPUT AND OUTPUT OF TESTS WITH FLYWHEEL 3200 GRAMS MASS

No	Input (Flywheel Disc)			Output			
	$m$ (gram)	$d$ (mm)	rpm	Inertia (kgm <sup>2</sup> )	Kinetic energy (J)	Centrifugal force	
				$I$ $= \frac{1}{2}mr^2$	$E_k$ $= \frac{1}{2}I\omega^2$	Newtons	kg
1	3200	200	100	0.016	0.877	35.1	3.57
2	3200	200	200	0.016	3.51	140.4	14.317
3	3200	200	300	0.016	7.89	315.91	32.21
4	3200	200	400	0.016	14.04	702.02	71.586
5	3200	200	500	0.016	21.938	877.53	89.48
6	3200	200	600	0.016	31.59	1263.6	128.56
7	3200	200	700	0.016	42.99	1720	175.39
8	3200	200	800	0.016	56.162	2246.5	229.08
9	3200	200	900	0.016	71.08	2843.2	289.92
10	3200	200	1000	0.016	87.75	3510.1	357.93
11	3200	200	1100	0.016	106.18	4247.2	433.1
12	3200	200	1200	0.016	126.36	5054.5	515.42
13	3200	200	1300	0.016	148.3	5932.1	604.9
14	3200	200	1400	0.016	172	6879.8	701.54
15	3200	200	1500	0.016	197.44	7897.7	805.34

The results of the indoor testing can be seen in Fig. 8(a). It shows a significant improvement in torque and power with the new 3.2 kg flywheel compared to the old 2.5 kg flywheel. The inclusion of a lithium battery also provided much better performance compared to relying on the fuel cell alone, allowing the vehicle to reach a top speed of 38.2 km/h. In contrast, when powered solely by the fuel cell, the speed only reached 30.2 km/h, with hydrogen pressure needing to be maintained at 30 psi. Additionally, Fig. 8(a) demonstrates that the flywheel played a crucial role in stabilizing the fuel cell's operation at 30 psi, helping to prevent intermittent power drops and ensuring smoother performance.

### B. The Electric Trike Vehicle Performance

The trike's gross weight has been optimized to approximately 75 kg, which is essential for enhancing its

performance and efficiency. This weight accommodated a driver weighing 65 kg, bringing the total load capacity to 140 kg. This careful consideration of weight is crucial for ensuring that the trike can effectively navigate various terrains, particularly on community roads that often feature inclines. With a design that allows it to traverse an average slope of 10 degrees, the designed trike demonstrated its capability to handle everyday challenges encountered in urban environments.

Extensive outdoor road testing has validated the vehicle's operational effectiveness, revealing that it could climb hilly terrain without encountering significant obstacles. This is an important characteristic, as many electric vehicles struggle with steep inclines due to their weight and power constraints [34]. The trike's design incorporated an efficient energy utilization strategy, allowing it to achieve higher speeds, smooth acceleration, and enhanced torque. These performance enhancements were made possible through the integration of a flywheel, which stores kinetic energy and provides additional power during acceleration, thereby improving overall responsiveness.

In the latest prototype, the trike was equipped with two-cylinder containers, each capable of storing 500 liters of ultra-high purity (UHP) hydrogen at a pressure of 2000 psi. This design choice is significant, as the high storage capacity and pressure ensure that the vehicle has sufficient fuel for extended journeys. The trike could achieve an average maximum speed of 30 km/h, which is ideal for urban commuting and community road use. To support this performance, it required 500 W hours of energy for a journey of approximately 30 km, demonstrating its efficiency in energy consumption relative to the distance travelled. Overall, this combination of lightweight design, effective energy management, and advanced hydrogen storage technology positions the trike as a viable option for sustainable transportation, particularly in settings where efficient and practical mobility solutions are essential.

### C. Fuel Cells Performance

The measurements conducted under no-load conditions revealed that the fuel cell produced an output voltage of approximately 59-61 V, compared to its nominal voltage of 48 V. Serial tests were also performed with the BLDC motor under load to assess the fuel cell's performance at various pressures, with the trike's top speed recorded. The results, significantly influenced by the flywheel rotation, are illustrated in Fig. 8(b). As shown in Fig. 8(b), at the lowest hydrogen pressure of seven psi, the fuel cell maintained an output of around 59 V under no-load conditions. However, when the throttle was turned up and the BLDC motor engaged, the voltage dropped due to the fuel cell's characteristics. The current measurement only showed six amperes, and with a smooth throttle application, the speed reached approximately 16.8 km/h. Increasing the throttle further led to an automatic cut-off of the fuel cell. Furthermore, it is noticeable that increasing the hydrogen pressure from 10 to 30 psi resulted in an increase in speed. The 30 psi condition was the highest pressure tested for safety, yielding an output of 597 W, exceeding the fuel cell's nominal power, with a maximum speed of about 30 km/h.

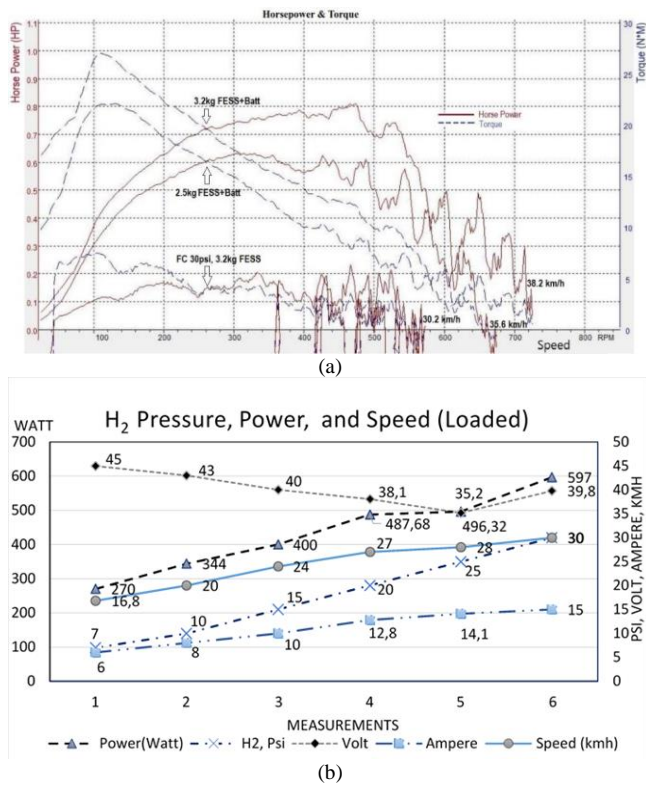


Fig. 8. (a) Indoor tests trike performance result and (b) Fuel cell performance with BLDC load



Fig. 9. (a) Route of outdoor test around B. J. Habibie Science and Technology Park, Serpong and (b) Speed, distance, and road altitude profile of outdoor testing.

Those results above mean that operating the trike solely on the fuel cell requires careful throttle management. An abrupt adjustment can cause the voltage to drop below the BLDC motor's operational range, triggering the fuel cell's protection system and leading to cut-off. However, Figure 8a

demonstrates that the use of a 3.2 kg flywheel could mitigate these interruptions, allowing the trike to operate at 30 km/h without battery support at 30 psi. Moreover, Figure 8a indicates that with a 3.2 kg flywheel and a battery, the trike could achieve speeds of 38.2 km/h, while a lighter 2.5 kg flywheel yields a maximum speed of 35.6 km/h. Consequently, the mass of the flywheel is of paramount importance; if it is excessively light, it will not offer substantial advantages, whereas if it is excessively heavy, it may result in energy wastage during startup. Hence, the selection of a 3.2 kg flywheel for the 500 Watt BLDC motor and the 75 kg vehicle weight appears to be appropriate for this experiment. Noting that, based on the experimental results, for maximum power output of 500 Watt, the trike consumed about two liters of hydrogen per minute. This means that to complete a 30 km trip, it requires 500 Wh of energy, translating to 120 liters of hydrogen at 30 psi. Therefore, a total of 500 liters of hydrogen can facilitate a journey of approximately 125 km.

#### D. Lithium Battery Storage Performance

In this study, a lithium battery storage system was designed with an energy capacity of 573.3 Wh (54.2V/10.5Ah), enabling a 500 W BLDC motor to achieve a maximum acceleration speed of 35.9 km/h. Noting that, as shown in Figs. 9a and 9b, the outdoor tests were performed on a slightly hilly concrete road with moderate slopes, rather than on a flat surface, inside B. J. Habibie Science Park and Technology area. The weather was clear, sunny and warm with 30° celcius of temperature, and 80% of humidity. Fig. 9b illustrates the outdoor testing parameters for the trike with battery energy storage, detailing speed, distance, and road altitude/slope. During outdoor testing, the trike reached speeds of up to 36.5 km/h, slightly exceeding the motor's maximum acceleration speed. The battery allowed the trike to cover approximately 15-20 km, translating to about 30 minutes of travel, indicating that solely relying on battery storage is not suitable for long-distance journeys. Therefore, implementing a hybrid storage system from PEMFC, flywheel, and battery is crucial to enhance the electric trike's capacity for extended travel. The battery can rapidly supply energy to boost the vehicle's speed (see Fig. 9b) because of its ability to deliver short bursts of power during peak loads [14]. In contrast, the PEMFC provides long-term energy, while the flywheel facilitates quick energy absorption and release, particularly during regenerative braking and other transient conditions, as discussed in sub section C about Fuel Cell Performance.

#### IV. CONCLUSION

Two EVs trike prototype platforms were developed for this research based on simulation design, featuring flywheels with masses of 2.5 kg and 3.2 kg, and diameters of 18 cm and 20 cm, respectively. The prototypes incorporated a 500 W fuel cell system and a 573.3 Wh lithium battery, which work together as multiple power sources to drive a 500 W, 48 V BLDC hub motor.

The trike's gross weight has been minimized to approximately 75 kg, accommodating a driver weighing 65 kg, resulting in a total load capacity of 140 kg. This configuration allowed the trike to navigate an average slope

of 10 degrees on community roads. Road testing has demonstrated that the vehicle operated effectively without encountering obstacles when climbing hilly terrain. The design efficiently utilized energy, achieving higher speeds, smooth acceleration, and improved torque through the integration of the flywheel.

The latest prototype featured two-cylinder containers, each capable of storing 500 liters of ultra-high purity (UHP) hydrogen at 2000 psi. The trike achieved an average maximum speed of 30 km/h, requiring 500 Wh of energy for a journey of approximately 30 km. The fuel cell stack consumed two standard liters per minute of hydrogen at 30 psi, resulting in a consumption of 120 liters of hydrogen per hour. Consequently, each 500-liter container could supply energy for 125 km, and both containers could extend the range to 250 km.

In spite of the inherent characteristics of the fuel cell stack and the centrifugal force generated by the flywheel, the second platform, equipped with a 3.2 kg flywheel operating at around 600 rpm, enhanced the fuel cell's capability to deliver power without interruption. This setup allowed the trike to reach speeds of up to 38.2 km/h without drawing energy from the battery. However, during initial acceleration, battery power is preferred until the vehicle attains a speed greater than 15 km/h, at which point the contributions from the fuel cell and flywheel optimize overall performance.

This research provides valuable insights into the effective utilization of a multi-energy storage system comprising a fuel cell, flywheel, and battery in an electric trike vehicle. Such an approach can optimize energy requirements for lightweight electric vehicles, supporting sustainable transportation solutions for daily activities, or to be used as a platform vehicle for: land manned drone, robotic survey vehicles, remote controlled vehicles, and autonomous vehicles, particularly in developing countries.

#### ACKNOWLEDGMENT

The first author expresses their sincere gratitude for the scholarship provided by the National Research and Innovation Agency (BRIN) of the Republic of Indonesia. The authors are honored to have had access to all BRIN laboratory facilities and testing equipment throughout the duration of this work from 2022 to 2023, which enabled the development of electric vehicle prototypes and the successful completion of this experiment. This research was funded under S.K. Ka.Brin; no. 12/III.3/HK/2022 (list no. 27), allowing us to conduct tests within the BRIN research centers area. The first author would like to extend special thanks to Professor Dr. Heri Suryoatmojo, Dr. Barman Tambunan, Dr. Tata Sutardi, and Dr. Taurista Perdana Syawitri, for their invaluable encouragement and support.

#### REFERENCES

- [1] H. Jing, Y. Chen, M. Ma, W. Feng, and X. Xiang, "Global carbon transition in the passenger transportation sector over 2000–2021," *Sustainable Production and Consumption*, vol. 51, pp. 556–571, 2024, doi: 10.1016/j.spc.2024.10.006.
- [2] L. A. S. Tayo *et al.*, "Performance Characterization of a Developed Battery Electric Tricycle," *2023 IEEE Transportation Electrification Conference and Expo, Asia-Pacific (ITEC Asia-Pacific)*, pp. 1–6, 2023, doi: 10.1109/ITECAsia-Pacific59272.2023.10372293.
- [3] A. L. C. Nacion, R. B. Dimla, and D. D. Soriano, "An Operational Efficiency Assessment of E-Trike and Motorized Tricycles as Public Utility Vehicles," *International Journal of Engineering and Advanced Technology*, vol. 12, no. 1, pp. 76–81, 2022, doi: 10.35940/ijeat.a3855.1012122.
- [4] F. Arifurrahman, Indrawanto, B. A. Budiman and S. P. Santosa, "Static Analysis of an Electric Three-Wheel Vehicle," *2018 5<sup>th</sup> International Conference on Electric Vehicular Technology (ICEVT)*, pp. 218–223, 2018, doi: 10.1109/ICEVT.2018.8628426.
- [5] B. Ramasubramanian, J. Ling, R. Jose, and S. Ramakrishna, "Ten major challenges for sustainable lithium-ion batteries," *Cell Rep. Phys. Sci.*, pp. 102032–102032, 2024, doi: 10.1016/j.xcrp.2024.102032.
- [6] N. A. A. Qasem, "A recent overview of proton exchange membrane fuel cells: Fundamentals, applications, and advances," *Appl. Therm. Eng.*, vol. 252, pp. 123746–123746, 2024, doi: 10.1016/j.applthermaleng.2024.123746.
- [7] F. Rahim Malik, H.-B. Yuan, J. C. Moran, and N. Tippayawong, "Overview of hydrogen production technologies for fuel cell utilization," *Engineering Science and Technology, an International Journal*, vol. 43, p. 101452, 2023, doi: 10.1016/j.jestch.2023.101452.
- [8] T. Gao, Y. Huang, X. Zhang, Z. Ma, and Y. Peng, "Optimization and mass transfer analysis under the ribs of multi-serpentine flow fields," *Engineering Science and Technology an International Journal*, vol. 55, pp. 101755–101755, 2024, doi: 10.1016/j.jestch.2024.101755.
- [9] Z. Wang, Z. Liu, L. Fan, Q. Du, and K. Jiao, "Application progress of small-scale proton exchange membrane fuel cell," *Energy Reviews*, vol. 2, no. 2, p. 100017, 2023, doi: 10.1016/j.enrev.2023.100017.
- [10] D. M. Nguyen, M. A. Kishk, and M.-S. Alouini, "Dynamic charging as a complementary approach in modern EV charging infrastructure," *Sci. Rep.*, vol. 14, no. 1, p. 5785, 2024, doi: 10.1038/s41598-024-55863-3.
- [11] M. M. Tellez-Cruz, J. Escorihuela, O. Solorza-Feria, and V. Compañ, "Proton Exchange Membrane Fuel Cells (PEMFCs): Advances and Challenges," *Polymers*, vol. 13, no. 18, p. 3064, 2021, doi: 10.3390/polym13183064.
- [12] X. Lü, Y. Qu, Y. Wang, C. Qin, and G. Liu, "A comprehensive review on hybrid power system for PEMFC-HEV: Issues and strategies," *Energy Convers. Manage.*, vol. 171, pp. 1273–1291, 2018, doi: 10.1016/j.enconman.2018.06.065.
- [13] Z. Aslam, A. Felix, C. Kalyvas, and Mahmoud Chizari, "Design of a Fuel Cell/Battery Hybrid Power System for a Micro Vehicle: Sizing Design and Hydrogen Storage Evaluation," *Vehicles*, vol. 5, no. 4, pp. 1570–1585, 2023, doi: 10.3390/vehicles5040085.
- [14] S. Zhao *et al.*, "Towards high-energy-density lithium-ion batteries: Strategies for developing high-capacity lithium-rich cathode materials," *Energy Storage Materials*, vol. 34, pp. 716–734, 2021, doi: 10.1016/j.ensm.2020.11.008.
- [15] V. Ramya and R. Marimuthu, "A review on multi-input converters and their sources for fast charging of electric vehicles," *Engineering Science and Technology an International Journal*, vol. 57, pp. 101802–101802, 2024, doi: 10.1016/j.jestch.2024.101802.
- [16] A. Urooj and A. Nasir, "Review of Hybrid Energy Storage Systems for Hybrid Electric Vehicles," *World Electric Vehicle Journal*, vol. 15, no. 8, pp. 342–342, 2024, doi: 10.3390/wevj15080342.
- [17] S. Verma *et al.*, "A comprehensive review on energy storage in hybrid electric vehicle," *Journal of Traffic and Transportation Engineering (English Edition)*, vol. 8, no. 5, pp. 621–637, 2021, doi: 10.1016/j.jtte.2021.09.001.
- [18] R. E. Kassar, A. A. Takash, J. Faraj, M. Hammoud, M. Khaled, and H. S. Ramadan, "Recent advances in lithium-ion battery integration with thermal management systems for electric vehicles: A summary review," *Journal of Energy Storage*, vol. 91, pp. 112061–112061, 2024, doi: 10.1016/j.est.2024.112061.
- [19] M. Amiray and K. Pullen, "A Review of Flywheel Energy Storage System Technologies and Their Applications," *Appl. Sci.*, vol. 7, no. 3, p. 286, 2017, doi: 10.3390/app7030286.
- [20] Z. Zhang, B. Yang, Y. Zhang, L. Li, B. Zhao, and T. Zhang, "Powertrain modeling and performance simulation of a novel flywheel hybrid electric vehicle," *Energy Reports*, vol. 9, pp. 4401–4412, 2023, doi: 10.1016/j.egy.2023.03.098.

- [21] S. Hoodorozhkov, "The flywheel energy storage for cargo bicycles," *MATEC Web of Conferences*, vol. 245, p. 07012, 2018, doi: 10.1051/mateconf/201824507012.
- [22] S. Wicki and E. G. Hansen, "Clean energy storage technology in the making: An innovation systems perspective on flywheel energy storage," *J. Cleaner Prod.*, vol. 162, pp. 1118–1134, 2017, doi: 10.1016/j.jclepro.2017.05.132.
- [23] M. Hedlund, J. Lundin, J. de Santiago, J. Abrahamsson, and H. Bernhoff, "Flywheel Energy Storage for Automotive Applications," *Energies*, vol. 8, no. 10, pp. 10636–10663, 2015, doi: 10.3390/en81010636.
- [24] S. M. Mousavi G, F. Faraji, A. Majazi, and K. Al-Haddad, "A comprehensive review of Flywheel Energy Storage System technology," *Renewable Sustainable Energy Rev.*, vol. 67, pp. 477–490, 2017, doi: 10.1016/j.rser.2016.09.060.
- [25] B. H. Kim, O. J. Kwon, J. S. Song, S. H. Cheon, and B. S. Oh, "The characteristics of regenerative energy for PEMFC hybrid system with additional generator," *Int. J. Hydrogen Energy*, vol. 39, no. 19, pp. 10208–10215, 2014, doi: 10.1016/j.ijhydene.2014.03.200.
- [26] G. T. Chandrasa, B. Tambunan and Soedibyo, "Design and Testing a Lightweight Electric Trike with Triple Hybrid Power Sources," *2022 7th International Conference on Electric Vehicular Technology (ICEVT)*, pp. 122–127, 2022, doi: 10.1109/ICEVT55516.2022.9924753.
- [27] S. K. Pradhan and B. Chakraborty, "Battery management strategies: An essential review for battery state of health monitoring techniques," *Journal of Energy Storage*, vol. 51, p. 104427, 2022, doi: 10.1016/j.est.2022.104427.
- [28] K. Fauziah *et al.*, "Performance Test of 1 kW PEM Fuel Cell System to Determine Its Empirical Model," *Evergreen: Jt. J. Novel Carbon Resour. Sci. Green Asia Strategy*, vol. 10, no. 3, pp. 1982–1990, 2023, doi: 10.5109/7151761.
- [29] Q. Meyer, C. Yang, Y. Cheng, and C. Zhao, "Overcoming the Electrode Challenges of High-Temperature Proton Exchange Membrane Fuel Cells," *Electrochem. Energy Rev.*, vol. 6, no. 1, p. 6, 2023, doi: 10.1007/s41918-023-00180-y.
- [30] S. Ajayan and A. I. Selvakumar, "Modeling and Simulation of PEM Fuel Cell Electric Vehicle with Multiple Power Sources," *International Journal of Recent Technology and Engineering (IJRTE)*, vol. 8, no. 6, pp. 2277–3878, 2020, doi: 10.35940/ijrte.F8420.038620.
- [31] F. Grumm, M. Schumann, C. Cosse, M. Plenz, A. Lücken, and D. Schulz, "Short Circuit Characteristics of PEM Fuel Cells for Grid Integration Applications," *Electronics*, vol. 9, no. 4, p. 602, 2020, doi: 10.3390/electronics9040602.
- [32] M. Derbeli, O. Barambones, and L. Sbita, "A Robust Maximum Power Point Tracking Control Method for a PEM Fuel Cell Power System," *Appl. Sci.*, vol. 8, no. 12, p. 2449, 2018, doi: 10.3390/app8122449.
- [33] K. Aydin and M. T. Aydemir, "Sizing design and implementation of a flywheel energy storage system for space applications," *Turkish Journal of Electrical Engineering & Computer Sciences*, vol. 24, pp. 793–806, 2016, doi: 10.3906/elk-1306-206.
- [34] D. Hu *et al.*, "A review of flywheel energy storage rotor materials and structures," *Journal of Energy Storage*, vol. 74, pp. 109076–109076, 2023, doi: 10.1016/j.est.2023.109076.
- [35] S. Lacock, A. A. du Plessis, and M. J. Booysen, "Electric Vehicle Drivetrain Efficiency and the Multi-Speed Transmission Question," *World Electric Vehicle Journal*, vol. 14, no. 12, p. 342, 2023, doi: 10.3390/wevj14120342.
- [36] Y. Elmasry, I. B. Mansir, Z. Abubakar, A. Ali, S. Aliyu, and K. Almamun, "Electricity-hydrogen nexus integrated with multi-level hydrogen storage, solar PV site, and electric-fuelcell car charging stations," *International Journal of Hydrogen Energy*, vol. 76, pp. 160–171, 2024, doi: 10.1016/j.ijhydene.2024.02.222.
- [37] J. Xu, C. Zhang, Z. Wan, X. Chen, S. H. Chan, and Z. Tu, "Progress and perspectives of integrated thermal management systems in PEM fuel cell vehicles: A review," *Renewable and Sustainable Energy Reviews*, vol. 155, p. 111908, 2022, doi: 10.1016/j.rser.2021.111908.
- [38] A. Draz, H. Ashraf, and P. Makeen, "Artificial intelligence computational techniques of flywheel energy storage systems integrated with green energy: A comprehensive review," *e-Prime - Advances in Electrical Engineering, Electronics and Energy*, vol. 10, p. 100801, 2024, doi: 10.1016/j.prime.2024.100801.
- [39] N. Prabhu, R. Thirumalaivasan, and B. Ashok, "Design of sliding mode controller with improved reaching law through self-learning strategy to mitigate the torque ripple in BLDC motor for electric vehicles," *Computers and Electrical Engineering*, vol. 118, p. 109438, 2024, doi: 10.1016/j.compeleceng.2024.109438.
- [40] M. Ishikawa, H. Kawai, Y. Kushima, T. Murao, K. Hirata, and M. Kishitani, "Tracking Control for FES Alternate Knee Bending and Stretching Trike With Electric Motor Assistance," *IFAC-PapersOnLine*, vol. 56, no. 2, pp. 3636–3641, 2023, doi: 10.1016/j.ifacol.2023.10.1526.
- [41] Y. Takata *et al.*, "FES-Assisted Standing-up Motion Control Incorporating Center of Mass Motion," *IECON 2023- 49th Annual Conference of the IEEE Industrial Electronics Society*, pp. 1–6, 2023, doi: 10.1109/IECON51785.2023.10312623.
- [42] C. Sun, M. Gao, H. Cai, F. Xu, and C. Zhu, "Data-driven state-of-charge estimation of a lithium-ion battery pack in electric vehicles based on real-world driving data," *Journal of Energy Storage*, vol. 101, p. 11398, 2024, doi: 10.1016/j.est.2024.113986.
- [43] A. Sadar, M. Amir, and N. Mohammad, "An optimal design of battery thermal management system with advanced heating and cooling control mechanism for lithium-ion storage packs in electric vehicles," *Journal of Energy Storage*, vol. 99, p. 113421, 2024, doi: 10.1016/j.est.2024.113421.
- [44] A. H. H. Ardakani and F. Abdollah, "A fast balance optimization approach for charging enhancement of lithium-ion battery packs through deep reinforcement learning," *Journal of Energy Storage*, vol. 89, p. 111755, 2024, doi: 10.1016/j.est.2024.111755.
- [45] T. Talluri, A. Angani, K. J. Shin, M.-H. Hwang, and H.-R. Cha, "A novel design of lithium-polymer pouch battery pack with passive thermal management for electric vehicles," *Energy*, vol. 304, p. 132205, 2024, doi: 10.1016/j.energy.2024.132205.
- [46] T.-F. Yang, P.-Y. Lin, C.-Y. Lin, W.-M. Yan, and S. Rashidi, "Study on thermal aspects of lithium-ion battery packs with phase change material and air cooling system," *Case Studies in Thermal Engineering*, vol. 53, p. 103809, 2024, doi: 10.1016/j.csite.2023.103809.
- [47] P. D. Giorgio, G. D. Ilio, E. Jannelli, and F. V. Conte, "Numerical analysis of an energy storage system based on a metal hydride hydrogen tank and a lithium-ion battery pack for a plug-in fuel cell electric scooter," *International Journal of Hydrogen Energy*, vol. 48, no. 9, pp. 3552–3565, 2023, doi: 10.1016/j.ijhydene.2022.10.205.
- [48] G. Lee, J. Song, J. Han, Y. Lim, and S. Park, "Study on energy consumption characteristics of passenger electric vehicle according to the regenerative braking stages during real-world driving conditions," *Energy*, vol. 283, p. 128745, 2023, doi: 10.1016/j.energy.2023.128745.
- [49] V. P. Dhote, M. M. Lokhande, and S. C. Gupta, "Test bench setup for emulating electric vehicle on-road conditions," *Energy Reports*, vol. 9, pp. 218–222, 2023, doi: 10.1016/j.egy.2023.05.145.
- [50] P. Halder *et al.*, "Advancements in hydrogen production, storage, distribution and refuelling for a sustainable transport sector: Hydrogen fuel cell vehicle," *International Journal of Hydrogen Energy*, vol. 52, pp. 973–1004, 2024, doi: 10.1016/j.ijhydene.2023.07.204.
- [51] R. Shan, J. Reagan, S. Castellanos, S. Kurtz, and N. Kittner, "Evaluating emerging long-duration energy storage technologies," *Renewable and Sustainable Energy Reviews*, vol. 159, p. 112240, 2022, doi: 10.1016/j.rser.2022.112240.
- [52] M. Elkholy, S. Schwarz, and M. Aziz, "Advancing renewable energy: Strategic modeling and optimization of flywheel and hydrogen-based energy system," *Journal of Energy Storage*, vol. 101, p. 113771, 2024, doi: 10.1016/j.est.2024.113771.
- [53] D. Huang, C. Jiao, and J. Fang, "Theoretical calculation and analysis of electromagnetic performance of high temperature superconducting electric flywheel energy storage system," *Physica C: Superconductivity and its Applications*, vol. 626, p. 1354599, 2024, doi: 10.1016/j.physc.2024.1354599.
- [54] N. Saberi, M. A. V. Rad, K. Zamanpour, and A. Kasaeian, "Comparative techno-economic analysis of battery bank and integrated flywheel and generator in a hybrid renewable system under tropical climate," *Journal of Energy Storage*, vol. 103, p. 114145, 2024, doi: 10.1016/j.est.2024.114145.

- [55] B. Yang, S. Si, Z. Zhang, B. Gao, B. Zhao, H. Xu, and T. Zhang, "Fuzzy energy management strategy of a flywheel hybrid electric vehicle based on particle swarm optimization," *Journal of Energy Storage*, vol. 101, p. 114003, 2024, doi: 10.1016/j.est.2024.114003.
- [56] Q. Liu, W. Zhang, Z. Zhang, and Q. Qi, "A drive system global control strategy for electric vehicle based on optimized acceleration curve," *Energy*, vol. 248, p. 123598, 2022, doi: 10.1016/j.energy.2022.123598.
- [57] L. Küng, T. Büttler, G. Georges, and K. Boulouchos, "How much energy does a car need on the road?," *Applied Energy*, vol. 256, p. 113948, 2019, doi: 10.1016/j.apenergy.2019.113948.
- [58] L. T. Hieu, N. X. Khoa, and O. T. Lim, "An investigation on the effective performance area of the electric bicycle with variable key input parameters," *Journal of Cleaner Production*, vol. 321, p. 128862, 2021, doi: 10.1016/j.jclepro.2021.128862.
- [59] L. Manuguerra, F. Cappelletti, M. Rossi, and M. Germani, "Design of electric vehicles for Industry 4.0: the case of an Autonomous Mobile Robot," *Procedia CIRP*, vol. 120, pp. 980-985, 2023, doi: 10.1016/j.procir.2023.09.111.
- [60] G. Sara, G. Todde, D. Pinna, and M. Caria, "Evaluating an autonomous electric robot for real farming applications," *Smart Agricultural Technology*, vol. 9, p. 100595, 2024, doi: 10.1016/j.atech.2024.100595.
- [61] X. Hu and R. H. Assaad, "The use of unmanned ground vehicles (mobile robots) and unmanned aerial vehicles (drones) in the civil infrastructure asset management sector: Applications, robotic platforms, sensors, and algorithms," *Expert Systems with Applications*, vol. 232, p. 120897, 2023, doi: 10.1016/j.eswa.2023.120897.
- [62] H. Tang, Y. Wu, Y. Cai, F. Wang, Z. Lin, and Y. Pei, "Design of power lithium battery management system based on digital twin," *Journal of Energy Storage*, vol. 47, p. 103679, 2022, doi: 10.1016/j.est.2021.103679.
- [63] K. S. Randhawa, "Advanced ceramics in energy storage applications: Batteries to hydrogen energy," *Journal of Energy Storage*, vol. 98, p. 113122, 2024, doi: 10.1016/j.est.2024.113122.
- [64] J. Yao *et al.*, "Investigating thermal runaway propagation characteristics and configuration optimization of the hybrid lithium-ion battery packs," *International Journal of Heat and Mass Transfer*, vol. 233, p. 126021, 2024, doi: 10.1016/j.ijheatmasstransfer.2024.126021.
- [65] Z. Chen, Z. Li, and G. Chen, "Optimal configuration and operation for user-side energy storage considering lithium-ion battery degradation," *International Journal of Electrical Power & Energy Systems*, vol. 145, p. 108621, 2023, doi: 10.1016/j.ijepes.2022.108621.
- [66] L. Chang, C. Ma, C. Zhang, B. Duan, N. Cui, and C. Li, "Correlations of lithium-ion battery parameter variations and connected configurations on pack statistics," *Applied Energy*, vol. 329, p. 120275, 2023, doi: 10.1016/j.apenergy.2022.120275.
- [67] Y. Huang, L. Jiang, H. Chen, K. Dave, and T. Parry, "Comparative life cycle assessment of electric bikes for commuting in the UK," *Transportation Research Part D: Transport and Environment*, vol. 105, p. 103213, 2022, doi: 10.1016/j.trd.2022.103213.
- [68] H. S. Yun, S. K. Jeon, Y.-K. Lee, V. H. Dao, and S. H. Nahm, "Characterizing microstructural changes due to hydrogen embrittlement: Predicting mechanical properties according to hydrogen amount," *Materials Characterization*, vol. 219, p. 114574, 2025, doi: 10.1016/j.matchar.2024.114574.
- [69] K. Chen, J. Luo, and Y. Huang, "Impact of low temperature exposure on lithium-ion batteries: A multi-scale study of performance degradation, predictive signals and underlying mechanisms," *Chemical Engineering Journal*, vol. 503, p. 158260, 2024, doi: 10.1016/j.cej.2024.158260.
- [70] K. J. Galambos, A. B. Palomino-Hernández, V. C. Hemmelmayr, and B. Turan, "Sustainability initiatives in urban freight transportation in Europe," *Transportation Research Interdisciplinary Perspectives*, vol. 23, p. 101013, 2024, doi: 10.1016/j.trip.2023.101013.
- [71] M. Azad, W. J. Rose, J. H. MacArthur, and C. R. Cherry, "E-trikes for urban delivery: An empirical mixed-fleet simulation approach to assess city logistics sustainability," *Sustainable Cities and Society*, vol. 96, p. 104641, 2023, doi: 10.1016/j.scs.2023.104641.
- [72] G. K. Ayetor, I. Mbonigaba, and J. Mashele, "Feasibility of electric two and three-wheelers in Africa," *Green Energy and Intelligent Transportation*, vol. 2, no. 4, p. 100106, 2023, doi: 10.1016/j.geits.2023.100106.
- [73] F. Berger *et al.*, "Benchmarking battery management system algorithms - Requirements, scenarios and validation for automotive applications," *eTransportation*, vol. 22, p. 100355, 2024, doi: 10.1016/j.etrans.2024.100355.
- [74] L. T. Hieu and O. T. Lim, "A deep learning approach for optimize dynamic and required power in electric assisted bicycle under a structure and operating parameters," *Applied Energy*, vol. 347, p. 121457, 2023, doi: 10.1016/j.apenergy.2023.121457.
- [75] B. Xiang, S. Wu, T. Wen, H. Liu, and C. Peng, "Design, modeling, and validation of a 0.5 kWh flywheel energy storage system using magnetic levitation system," *Energy*, vol. 308, p. 132867, 2024, doi: 10.1016/j.energy.2024.132867.
- [76] Z. Zhang, B. Yang, Y. Zhang, L. Li, B. Zhao, and T. Zhang, "Powertrain modeling and performance simulation of a novel flywheel hybrid electric vehicle," *Energy Reports*, vol. 9, pp. 4401-4412, 2023, doi: 10.1016/j.egy.2023.03.098.
- [77] A. Ngendahayo, A. Junyent-Ferré, J. M. R. Bernuz, and E. Ntagwirumugara, "Itinerary-Dependent Degradation Analysis of a Lithium-Ion Battery Cell for E-Bike Applications in Rwanda," *Energy Engineering*, vol. 121, no. 11, pp. 3121-3131, 2024, doi: 10.32604/ee.2024.053100.
- [78] H. Yan, K. C. Marr, and O. A. Ezekoye, "Thermal runaway behavior of nickel-manganese-cobalt 18650 lithium-ion cells induced by internal and external heating failures," *Journal of Energy Storage*, vol. 45, p. 103640, 2022, doi: 10.1016/j.est.2021.103640.
- [79] K. C. Abbott *et al.*, "Experimental study of three commercially available 18650 lithium ion batteries using multiple abuse methods," *Journal of Energy Storage*, vol. 65, p. 107293, 2023, doi: 10.1016/j.est.2023.107293.
- [80] L. Zhao, J. Tong, M. Zheng, M. Chen, and W. Li, "Experimental study on the thermal management performance of immersion cooling for 18650 lithium-ion battery module," *Process Safety and Environmental Protection*, vol. 192, pp. 634-642, 2024, doi: 10.1016/j.psep.2024.10.057.